DOI:10.1190/segam2016-13950552.1

High resolution image-guided tomographic solution for improved imaging in ultrashallow water trench area of Gulf of Mexico

*Sandip Chattopadhyay *, Gary Rodriguez, Tefera Eshete, Guy Hilburn*
TGS, Houston, Texas

Summary

We present an improved depth imaging methodology, which utilizes a high-resolution image-guided tomographic solution that addresses the difficulties introduced by a highly unconsolidated slow velocity overburden, in this case a gas-charged mud-filled trench. The improved workflow allowed the replacement of long-period statics with a more accurate velocity model that solved for the slow velocity overburden. The resulting image yielded a better-focused image with more geologically plausible images. The project consists of 41 OCS blocks of data in the South Timbalier trench of the Gulf of Mexico.

The main objectives of this project were to address the ultrashallow water trench static problem and to produce a high-resolution velocity model. In this paper we present an enhanced depth imaging flow using full-azimuth, anisotropic, image-guided tomographic model building and depth imaging on long-offset, full-azimuth ocean-bottom acquisition.

Introduction

The project area is located in the ultrashallow water of the South Timbalier trench area of the Gulf of Mexico, which has complex static problems. The statics problem is often addressed in the time domain by applying time shifts from a refraction statics solution to the traces. In the depth domain, processing the same time shift when applied to the input data will produce kinematically incorrect depth migration results and can lead to velocity distortions during successive tomography-based model building (Rodriguez et al., 2009).

The statics problem is instead addressed in the depth domain by successive high-resolution tomography iterations. The long period statics that were previously applied to input data, were removed for depth migration. The high frequency nature of the surface consistent residual statics was difficult to resolve via tomographic inversion; this portion of the statics is instead applied to input data prior to depth migration.

The improved high-resolution depth images are produced by proper well-to-seismic calibration, anisotropic parameter estimation and multiazimuth tomographic inversion. The offset-dependent event picking and geologically constrained image-guided tomographic inversion further enhanced the image quality. The final depth imaging results demonstrated great uplift, with accurate images, improved image focusing, correctly positioned steeply dipping events and better well-to-seismic ties.

Survey area

The newly acquired 3D OBC covers 41 OCS blocks, located in the ultrashallow water in South Pelto/Grand Isle area of the Gulf of Mexico (Figure 1). The orthogonal acquisition used Sercel SeaRay ocean-bottom cable with long inline offset (16 km).

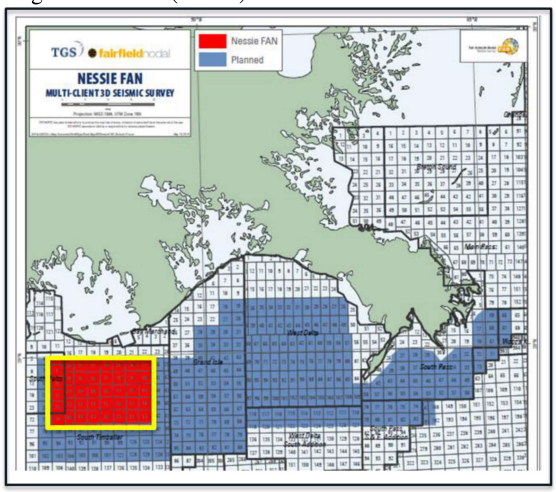

Figure 1. Survey location map of the project area.

Input data preprocessing

The data preparation includes deblending of sources, coherent and random noise attenuation, designature, short and long wavelength statics correction, wavefield separation (selecting the upgoing wavefield only), surface-consistent deconvolution, surface-consistent amplitude corrections and Q compensation.

The input data was divided into six azimuth sectors (-60^0, -30^0, 0^0, 30^0, 60^0, 90^0) and binned for multiazimuth model building and depth imaging as shown in Figure 2.

Initial anisotropic model building

The time-RMS model derived from PSTM velocity analysis was the starting velocity model for the project. The velocity model was converted to the depth-interval velocity

domain, and an isotropic shallow tomographic inversion was run before calibration with checkshots.

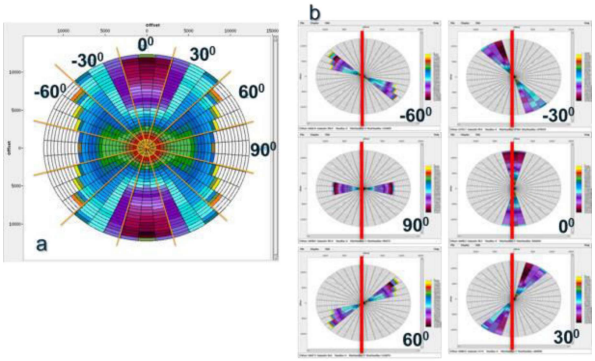

Figure 2. a) Offset-azimuth map (Rose diagram) of Nessie 3D data, b) Offset-azimuth distribution of individual azimuth sectored data for multiazimuth TTI model building. Red line represents receiver line direction.

Twenty-two checkshots are selected for calibration purposes. Anomalous trends are edited before using them for calibration. Scalar functions are derived at checkshot locations that would match the migration velocity to the checkshots.

These scalar functions are interpolated and extrapolated along key interpreted horizons. The fully interpolated scalar functions are used to produce a scalar grid to be used to match the migration velocity field to the checkshots.

Prestack depth migration is performed with the calibrated velocity model. Since there was a lack of checkshot information in the trench area, the velocity model did not reflect the low velocity trend that was present in the trench.

This lack of slow velocities resulted in a migrated image with a significant structural sag (Figure 3).

In an effort to speed the process and ensure tomographic velocity convergence, a slow velocity trend is manually inserted in the trench area. A constant velocity value of 1350 m/s is inserted in the region between the water bottom and an interpreted base of trench. Successive iterations of high-resolution shallow tomography would further refine the velocity model in this region. Outside of the trench the previously calibrated model was used as an initial vertical velocity model V_z for the subsequent model building process.

An isotropic Kirchhoff prestack depth migration is run using the resulting V_z model. Since the model matched the checkshot velocities at checkshot locations, residual moveout at these locations is attributed to anisotropy.

Therefore, common image gathers (CIGs) at the checkshot locations were then fed to a Focusing Analysis (Cai et al., 2009) tool to derive anisotropic parameters δ and ε (Thomsen, 1986) at the well locations.

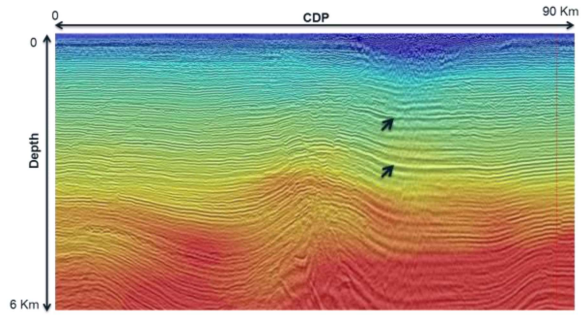

Figure 3. The initial calibrated model shows depth-sag due to removing long-period statics from the input data prior to depth imaging.

These ε and δ values are edited and smoothed to identify a general trend for the study area. Since the project area was relatively small, a single ε and δ function is sufficient for the entire area

To this end a single average function, which best represented the anisotropic function in the study area was derived. This function is extrapolated along the previously interpreted horizons to generate fully populated ε and δ volumes for the successive anisotropic model building and depth imaging processes.

TTI model building

The initial V_z model and the derived anisotropic parameters are used to convert vertical velocity V_z to normal velocity V_0 for anisotropic depth migration. The initial 3D dip fields (in the x-direction and y-direction) are generated from an isotropically migrated stacked image volume and fed into the TTI depth migration flow.

The Tilted Transverse Isotropic (TTI) model updating is done in two steps, a) shallow trench tomography and b) deeper high-resolution image-guided tomography (IGT).

Shallow trench tomography

The 3D OBC data is then azimuthally sectored, during the binning process, to ensure the full azimuthal illumination of the study area. The input data is sectored into six azimuths (Figure 2). Each of these azimuths was migrated using TTI prestack Kirchhoff depth migration. To ensure a high-resolution model update at very shallow depths and in the trench area, a finer tomographic inversion grid is adopted. Single parameter curvature-based residual moveout (RMO) is picked on scanned semblances derived from TTI PSDM CIGs. We noted that a positive curvature (increasing

reflection depth with increasing offset) was picked in the trench area, which would translate into an implied velocity decrease. This velocity slowdown is consistent with what is expected for unconsolidated gas charged mud (Tóth et al., 2014). Velocities as low as 1000 m/s resulted after two tomographic updates (Figure 4 and 5).

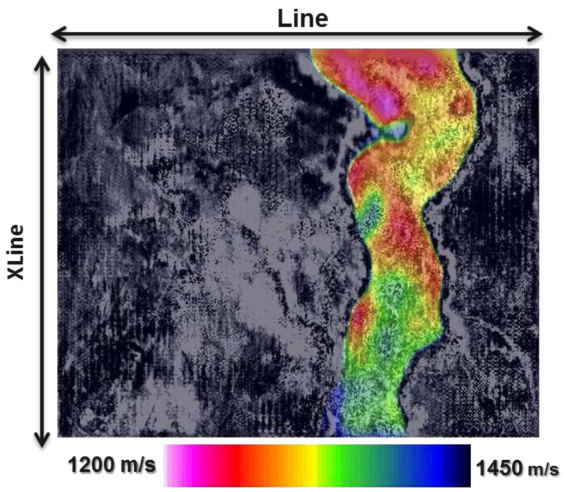

Figure 4. Velocity update at 300 m depth. The color bar is restricted to show velocity values only in the trench area. Low velocity (~ 1000 m/s) was observed in the South Timbalier trench area.

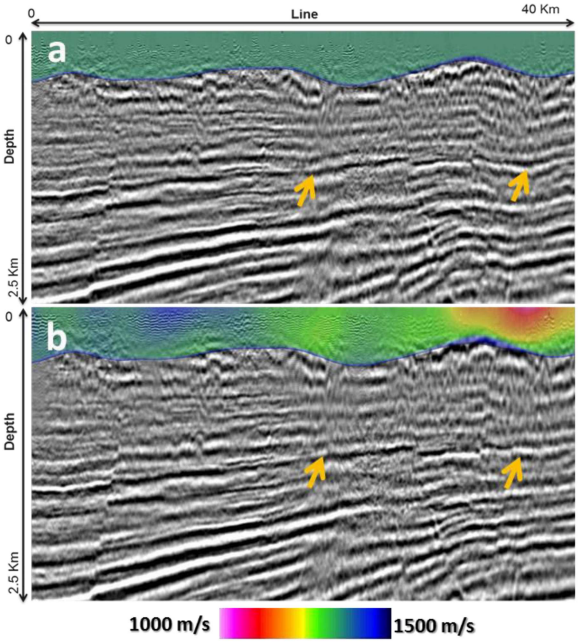

Figure 5. Velocity update in the trench area. a) Initial model and b) after shallow tomography update in the trench area. The color bar is restricted to show velocity values only in the trench area. The arrows show that velocity update in the trench area helped to improve image quality and diminish structural sag.

The tomographic updates not only better flattened the CIGs, but dramatically diminished the structural sag (Figure 5). Additionally, faults are better focused, all of which gave more confidence that the velocity updates were converging towards a correct velocity model.

High-resolution, image-guided tomography update

A higher resolution model update was achieved by offset-dependent RMO picking and image-guided tomography (IGT). (Hale, 2009; Hilburn et.al., 2014).

Offset-dependent picking is a robust process utilizing an event-finding technique which is guided by analyzing amplitude variation between traces in the CIGs, geological dips, continuity of the reflector, displacement of events within gathers and a required flatness-constraint (Hilburn et al., 2014). This procedure honors events with complex moveout patterns better. More accurately sampling the residual depth error should also allow for better resolution in the velocity model.

To obtain a geologically-conformable solution, structurally constrained IGT inversion is applied to generate a model update. The directionality and continuity of events were used to calculate a set of tensors (Hale, 2009; Hilburn et al., 2014) that can be used to define update zones whose boundaries are computed by minimizing structure-oriented propagation time within the underlying image (Tiwari et al., 2015). Disruptions in this propagation time identify the coherent and incoherent structures (e.g. faults) (Hilburn et al., 2014). The zonal distribution, computed tensors and the propagation time combine to describe a preconditioning operator for the tomographic inversion (Hilburn et al., 2014; Tiwari et al., 2015).

For each azimuthal sector, the offset-dependent complex move out pattern is picked on previously-updated prestack depth migrated CIGs. A new dip field was computed on the updated stack volume to feed correct dip information into the IGT inversion. Multiazimuth ray tracing is performed to incorporate offset-dependent residual curvature and the newest dip field information. Multiazimuth ray tracing and IGT parameters are then fed into a final tomographic inversion for a geologically conformable model update. A higher resolution and geologically conformable image-guided tomography (IGT) update produces a higher resolution background sediment velocity model (Figure 6) for depth imaging.

The snail gathers (Lecerf et al., 2009) were generated to analyze azimuthal kinematic variation of CIGs. The snail gathers show (Figure 7), the wobbling effect has been greatly reduced and the flatness has been improved after combination of shallow trench tomography and high-resolution image-guided (IGT) tomography update.

DOI:10.1190/segam2016-13950552.1

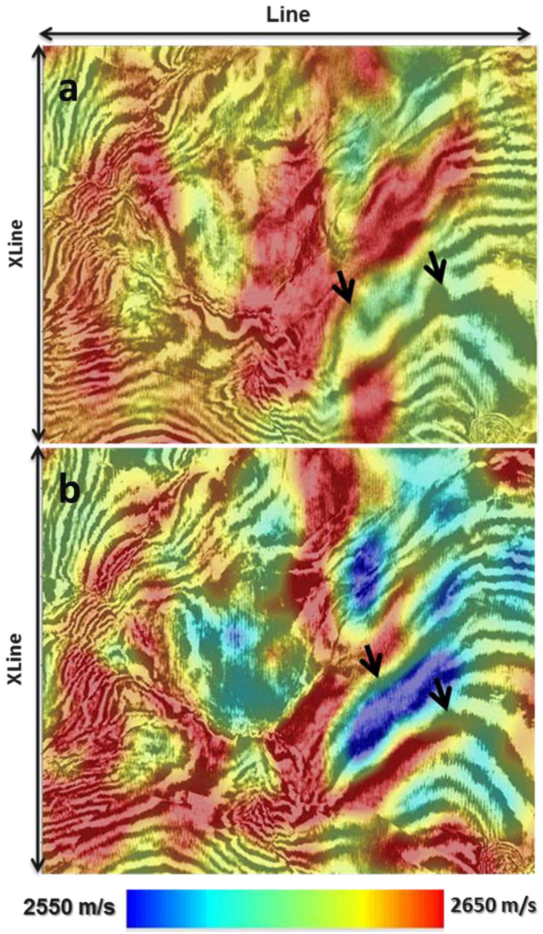

Figure 6. High-resolution, offset-dependent and image-guided tomography (IGT) update at 2500 m depth. The arrows shows improvement of image quality. a) PSDM depth slice with initial model and b) after shallow and high resolution tomography update. The IGT updated velocity follows underlying structure .

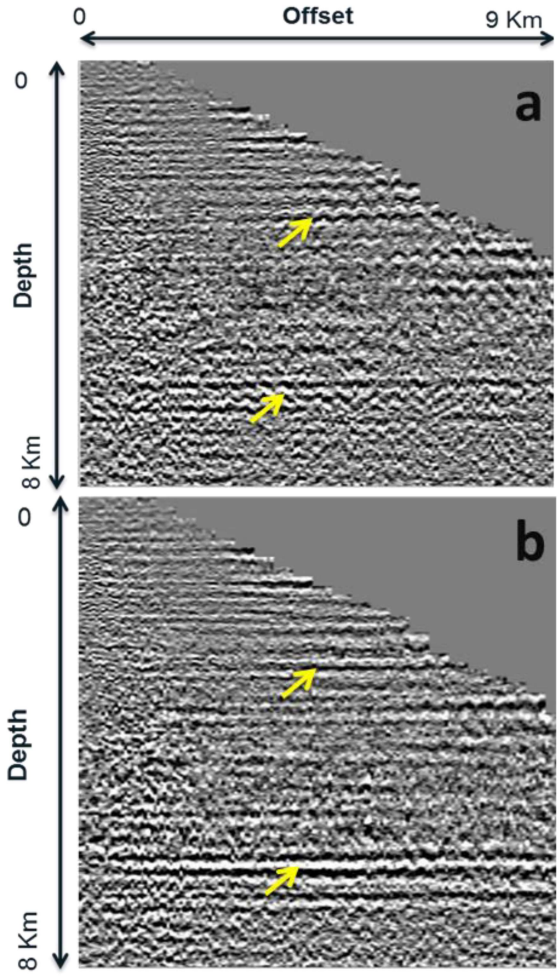

Figure 7. a) and b) show snail gathers with intial model and after high-resolution tomography update. The arrows show improvements after high resolution tomographic update.

Conclusions

The South Timbalier trench statics problem was addressed by shallow reflection tomography update rather than conventional refraction delay-time method. Offset-dependent picking and IGT tomography update resulted in higher resolution and a geologically conformable model update with a) better focused and improved subtrench events b) improved fault imaging in the whole project area.

Acknowledgements

We thank TGS management for permission to publish this paper. We thank Connie VanSchuyver for proofreading the manuscript. We would also like to thank Ashley Lundy, Kenny Lambert, George Cloudy Jr., Bin Wang, and Zhiming Li for their support and suggestions. The Nessie survey is a cooperative effort between TGS and Fairfield.

DOI:10.1190/segam2016-13950552.1

EDITED REFERENCES

Note: This reference list is a copyedited version of the reference list submitted by the author. Reference lists for the 2016 SEG Technical Program Expanded Abstracts have been copyedited so that references provided with the online metadata for each paper will achieve a high degree of linking to cited sources that appear on the Web.

REFERENCES

Cai, J., Y. He, Z. Li, B. Wang, and M. Guo, 2009, TTI/VTI anisotropy parameters estimation by focusing analysis, Part I: Theory: 79th Annual International Meeting, SEG, Expanded Abstracts, 301–305, http://dx.doi.org/10.1190/1.3255480.

Hale, D., 2009, Image-guided blended neighbor interpolation: CWP Report 634: Colorado School of Mines.

Hilburn, G., Y. He, Z. Yan, and F. Sherrill, 2014, High-resolution tomographic inversion with image-guided preconditioning and offset-dependent picking: 84th Annual International Meeting, SEG, Expanded Abstracts, 4768–4772, http://dx.doi.org/10.1190/segam2014-1219.1.

Lecerf, D., S. Navion, J. L. Boelle, A. Belmokhtar, and A. Ladmek, 2009, Azimuthal residual velocity analysis in offset vector for WAZ imaging: 71th Annual International Conference and Exhibition, EAGE, Extended Abstracts, V013.

Rodriguez, G., and S. Yang, D, Yang, Q, Zhang, and S. Hightower, 2009, Improved imaging through anisotropic depth migration and high resolution shallow tomography in lieu of refraction statics in South Timbalier trench area of Gulf of Mexico: A case history: 79th Annual International Meeting, SEG, Expanded Abstracts, 527–531, http://dx.doi.org/10.1190/1.3255812.

Thomsen, L., 1986, Weak elastic anisotropy: Geophysics, **51**, 1954–1966, http://dx.doi.org/10.1190/1.1442051.

Tiwari, D., G. Hilburn, Y. He, Y. Li, F. Sherrill, and Z. Guo, 2015, High resolution tilted-orthorhombic tomographic inversion to improve velocity modeling and imaging: A case study of its impact on subsalt: 85th Annual International Meeting, SEG, Expanded Abstracts, 361–365, http://dx.doi.org/10.1190/segam2015-5922279.1.

Tóth, Z., V. Spiess, J. M. Mogollón, and J. B. Jensen, 2014, Estimating the free gas content in Baltic Sea sediments using compressional wave velocity from marine seismic data: Journal of Geophysical Research. Solid Earth, **119**, 8577–8593, http://dx.doi.org/10.1002/2014JB010989.